

Reducing the risk of Atlantic thermohaline circulation collapse: sensitivity analysis of emissions corridors

Kirsten Zickfeld*

Potsdam Institute for Climate Impact Research, Potsdam, Germany

Thomas Bruckner

Institute for Energy Engineering, Technical University of Berlin, Berlin, Germany

Abstract

We present emissions corridors for the 21st century reducing the risk of collapse of the Atlantic thermohaline circulation (THC) while considering expectations about the socio-economically acceptable pace of emissions reductions. Emissions corridors embrace the range of CO₂ emissions that are compatible with normatively defined policy goals or ‘guardrails’. They are calculated along the conceptual and methodological lines of the tolerable windows approach. We investigate the sensitivity of the emissions corridors to key uncertain physical quantities (i.e. climate sensitivity and North Atlantic hydrological sensitivity, emissions of non-CO₂ greenhouse gases and sulfate aerosols) as well as to the guardrails. Results indicate a large dependency of the width of the emissions corridor on climate and hydrological sensitivity: for low values of the climate and/or hydrological sensitivity, the corridor boundaries are far from being transgressed by business-as-usual emissions scenarios for the 21st century. In contrast, for high

⁰Corresponding author: School of Earth and Ocean Sciences, University of Victoria, PO Box 3055 STN CSC, Victoria, BC, Canada, V8W3P6, E-mail: zickfeld@ocean.seos.uvic.ca

values of both quantities already low non-intervention scenarios leave the corridor in the early decades of this century. The width of the CO₂ emissions corridor is also affected by the emissions pathway of non-CO₂ greenhouse gases and sulfate aerosols, but to a lesser extent. We further find that the choice of the policy goal strongly influences the shape of the emissions corridor. Pursuit of a more ambitious THC target, for instance, tightens the corridor considerably. More strict expectations concerning the socio-economically admissible pace of emissions reduction (expressed in terms of a maximum emissions reduction rate and a transition time towards a de-carbonizing economy) act in the same direction. This indicates that a trade-off between THC and socio-economic guardrails may be unavoidable in the case of very tight emissions corridors. On the basis of our findings we conclude that ‘business-as-usual’ paths would need to be abandoned within the next decades, if the risk of THC collapse is to be kept low.

1 Introduction

The ultimate objective of climate change mitigation is to reduce the amount of anthropogenic greenhouse gas (GHG) emissions in order to achieve “stabilization of greenhouse gas concentrations in the atmosphere at a level that would prevent dangerous anthropogenic interference with the climate system” (UNFCCC, Article 2). Before being able to specify a stabilization target, scientists and policymakers are thus confronted with the challenging task of defining “what is dangerous” (Parry et al. 1996; Smith et al. 2001; Caldeira et al. 2003; Hansen 2005; Keller et al. 2005; Oppenheimer and Petsonk 2005; Oppenheimer and Alley 2005; Schellnhuber et al. 2006).

One interpretation has been offered by the Intergovernmental Panel on Climate Change (IPCC). In its Third Assessment Report (TAR) it developed a synthesis framework addressing five “reasons for concern”, which relate different categories of impacts to the respective level of climate change at which they are likely to occur (Smith et al. 2001). These include “damage to or irreparable loss of unique and threatened systems”, “distribution of impacts”, “global aggregated impacts”, “the probability of extreme weather events”, and “the probability of large-scale discontinuities”. The latter refers to events of regional or global scale that are brought about by nonlinear and threshold effects in the climate system. Here, we address the fifth reason for concern and explore climate policies to reduce the risk of “large scale discontinuities”. Specifically, we derive emissions corridors reducing the risk of a collapse of the Atlantic thermohaline circulation (THC), which is a prominent example of this category of impacts, while considering expecta-

tions about the socio-economically acceptable pace of emissions reduction efforts, in accordance with the goals of environmental and socio-economic sustainability put forward by Article 2 of the UNFCCC. It should be noted that many impacts of climate change, for instance those addressed by the other four reasons for concern, but also other large scale discontinuities such as melting of the Greenland ice sheet and disappearance of summer Arctic sea ice cover, are likely to be triggered at lower levels of climate change than a collapse of the thermohaline circulation (Holland et al. 2006; Gregory and Huybrechts 2006). Our study should therefore be interpreted as a contribution to an overall confinement strategy that intends to elucidate the various facets of “dangerous anthropogenic interference”.

The Atlantic thermohaline circulation (THC) transports large amounts of heat northward, contributing a major part to the heat budget of the North Atlantic region (Macdonald and Wunsch 1996). Evidence from paleoclimatic reconstructions (Dansgaard et al. 1993), theoretical considerations (Stommel 1961), and model simulations (Manabe and Stouffer 1988; Rahmstorf 1995; Rahmstorf et al. 2005) suggest that the thermohaline circulation system is subject to a nonlinear threshold dynamics switching into and out certain states where either the circulation breaks down completely or a shift in the location of deep water formation occurs.

Concerns have been raised that anthropogenic climate change might act as a trigger for such mode switches in the future. Model simulations in fact show the potential for THC instability under global warming scenarios. Manabe and Stouffer (1993), Stouffer and Manabe (2003) and Winguth et al. (2005) simulated a complete shutdown of the THC for a quadrupling

of atmospheric CO₂ concentrations. Stocker and Schmittner (1997) found a permanent shutdown of the THC under stabilization of CO₂ concentrations at 750 ppm. The ‘critical’ stabilization level was shown to be dependent on the rate at which the final CO₂ concentration level was attained. Under the assumption of a strong response of the hydrological cycle to GHG forcing, Rahmstorf and Ganopolski (1999) obtained the transition to the off state for a scenario with CO₂ concentrations peaking at around 1200 ppm in the 22nd century and declining thereafter. A regional shutdown of deep-water formation in the Labrador and the Greenland-Iceland-Norwegian (GIN) Sea was simulated by Wood et al. (1999) and Schaeffer et al. (2002) in the 21st century under ‘business-as-usual’ emissions scenarios (scenarios SRES A1b and IS92a, respectively). Of the comprehensive general circulation models (‘GCMs’) used in the IPCC Fourth Assessment Report none showed a complete shutdown in the 21st century (Gregory et al. 2005; Schmittner et al. 2005). Elicitations of subjective probability distributions from climate scientists, however, indicate higher probabilities of THC collapse than those reported in recent modelling studies (Zickfeld et al. 2007). The reason for this discrepancy is that people include in their probability estimates their own judgement about the skillfulness of climate models in representing relevant physical processes as well as information from sources other than modelling (e.g., observations, paleoclimatic reconstructions).

The consequences of a complete collapse of the THC for the climate of the North Atlantic region are highly uncertain. One reason is that estimates of the magnitude and the exact location of the cooling anomaly associated with a reduction of the oceanic heat transport differ widely between mod-

els. Vellinga and Wood (2002), for example, simulated a maximum mean annual cooling over the North Atlantic of 6 °C. In the model-intercomparison study by Stouffer et al. (2006) the ensemble mean maximum cooling after a shutdown of the THC is 12 °C. An outlier study even finds a cooling of up to 22 °C (Schiller et al. 1997). While in some models the maximum cooling is located over the western North Atlantic, in others (e.g. Vellinga and Wood 2002) it is centered over the eastern North Atlantic. Also, it is unclear to what extent the cooling would be compensated locally by greenhouse warming, as the net temperature response depends not only on the relative magnitude of the GHG and THC-induced temperature change, but also on their relative timing. Vellinga and Wood (2007), by investigating the climatic effects of THC collapse under GHG concentrations rising up to 700 ppm, find a slight net cooling over the North Atlantic relative to pre-industrial conditions. Transient model simulations reveal that a GHG induced collapse of the THC could lead to a reversal of the warming trend and a cooling by 2–3 °C (relative to the peak warming) within a few decades touching north-western Europe and north-eastern America (Rahmstorf and Ganopolski 1999). Vellinga and Wood (2002) have highlighted that the climatic consequences of a THC collapse may extend well beyond the North Atlantic. As a result of the change in cross-equatorial oceanic heat transport, for instance, the Intertropical Convergence Zone (ITCZ) would move southwards, with a consequent shift of tropical precipitation patterns, e.g. the Monsoons.

Worldwide changes in climate associated with a THC shutdown would affect the terrestrial biosphere and the services it provides, for example car-

bon storage. Higgins and Vellinga (2004) find that under pre-industrial CO₂ concentration a THC collapse would result in changes in ecosystem distribution and a global reduction in net primary production and biomass. Also, thermohaline circulation changes would affect the physical properties (e.g., temperature, mixed layer depth) of the North Atlantic waters, with possibly disruptive consequences for marine ecosystems and fisheries (Schmittner 2005; Vikebø et al. 2007). In turn, a reduction of the biological “carbon pump” (i.e. the process by which ocean biota remove CO₂ from surface waters and transport it to depth) together with changes in the physical mechanisms determining ocean carbon uptake (e.g. deep water formation) could lead to a significant reduction in the oceanic carbon sink (Obata 2007). Furthermore, studies by Levermann et al. (2005) and Vellinga and Wood (2007) suggest that a reorganization of the THC would bring about up to 0.5 m of sea level rise along North Atlantic coasts, both due to stronger heat storage in the deep ocean and dynamic effects.

Although a comprehensive assessment of the impacts of nonlinear THC changes is in its initial stage, there are indications that they could be severe. A collapse of the THC may thus well deserve the attribute of “dangerous anthropogenic interference with the climate system”. In this paper we present emissions corridors compatible with the goal of reducing the risk of THC collapse while considering expectations about the socio-economically acceptable pace of emissions reduction efforts. Emissions corridors represent the range of CO₂ emissions that are compatible with normatively defined policy goals or ‘guardrails’. They are calculated on the conceptual basis of the “tolerable windows approach” (TWA or “guardrail approach”; Bruckner et al.

1999; Petschel-Held et al. 1999). The TWA differs fundamentally from conventional integrated assessment approaches such as cost-benefit (Nordhaus 1994) or cost-effectiveness analysis (Manne et al. 1995), as it does not seek to identify a single ‘optimal’ emissions path, but the full range of emissions admitted under the pre-defined guardrails. We draw on the TWA as it offers several advantages compared to conventional cost-benefit analysis, particularly in the context of singular climate change (Schellnhuber 1997; Bruckner et al. 1999). Firstly, it is designed from the very beginning to account for nonlinear and threshold effects in the climate system. Secondly, it avoids the difficult aggregation across time, space and impact categories which is needed to value the benefits of avoided damages and compare them to the costs of climate protection. Thirdly, it allows for a clear separation of normative settings and rigorous scientific analysis. Mastrandrea and Schneider (2001), for example, have shown that optimal carbon taxes are extremely sensitive to the assumption made about the (normative) quantity expressing aggregation across time (i.e. the pure rate of time preference; cf. also Keller et al. 2000). The reason for this strong sensitivity lies in the inertia of the ocean which leads to a delay of the impacts with respect to the actual anthropogenic trigger by decades to centuries. Lastly, any analysis carried out on the basis of the TWA does not need the specification of a damage function. This is particularly valuable in the present context, since, as discussed above, we are far from being able to come up with a complete accounting of impacts associated with THC changes.

With one exception (Tóth et al. 1998), earlier attempts to explore the implications of nonlinear changes in the THC for climate change decision-

making were conducted in either a cost-benefit or cost-effectiveness framework (Nordhaus 1994; Lempert et al. 1994; Keller et al. 2000; Mastrandrea and Schneider 2001; Keller et al. 2004; Bahn et al. 2006; Yohe et al. 2006; Bahn et al. 2007). In the majority of these studies (except for Mastrandrea and Schneider 2001 and Yohe et al. 2006) an adapted version of the THC stability diagram derived by Stocker and Schmittner (1997) is applied as a constraint preventing a shutdown of the THC. This procedure, however, implies some drastic simplifications: it assumes that restrictions are imposed on the actual magnitude and rate of temperature change rather than on the asymptotic temperature change and the long-term average rate of change, although the latter were used to derive the stability curve. Mastrandrea and Schneider (2001) coupled a simple dynamic THC model iteratively to a model of the world economy. The first fully coupled modeling framework incorporating a dynamic representation of the THC was presented in Zickfeld and Bruckner (2003). The present paper is an extension of Zickfeld and Bruckner (2003) in that it presents a comprehensive sensitivity analysis taking into account key uncertainties, scientific as well as normative.

2 Methodological aspects

2.1 Modeling framework

The methodology applied for the scope of this paper will be described only briefly, as a detailed description is given elsewhere (Zickfeld and Bruckner 2003). In our analysis, we draw on the conceptual and methodological framework provided by the TWA. As mentioned in Section 1, the TWA is

an inverse approach which seeks to identify the bundle of emissions paths (the emissions corridor) that is compatible with pre-defined policy goals or guardrails. Here, we derive emissions corridors which are compatible with two kinds of guardrails. The first is environmentally motivated and aims at preventing ‘dangerous’ changes in the THC. The second is socio-economic in nature and is meant to limit the pace of GHG mitigation.

We use an integrated model (Zickfeld and Bruckner 2003) consisting of a dynamic four-box model of the Atlantic (Zickfeld et al. 2004) coupled to a globally-aggregated multi-gas climate model (ICM; Bruckner et al. 2003). This model setup allows us to represent the full causal chain from emissions of greenhouse gases (GHGs) and aerosols to THC strength, which is needed to translate the THC guardrail into the admissible range of emissions (i.e., the emissions corridor). Key uncertain quantities, such as the climate and North Atlantic hydrological sensitivity (i.e., a measure for the response of the hydrological cycle in the North Atlantic to climate change; Rahmstorf and Ganopolski 1999) are parameters in this model and can easily be varied. The energy-economy system is not modeled explicitly: the pertinent guardrails are implemented in a simplified way in the form of constraints on the emissions trajectory (Section 2.2; see also Kriegler and Bruckner 2004; Zickfeld and Bruckner 2003).

The algorithm for the computation of the upper (lower) boundary of an emissions corridor consists in subsequently maximizing (minimizing) energy related CO₂ emissions for fixed points in time t_i . The entire upper (lower) boundary is then put up by the maxima (minima) of such emissions paths (Leimbach and Bruckner 2001; Bruckner et al. 2003). For the corridors pre-

sented in this paper, the upper and lower boundaries are calculated for the period 2000–2100 in time steps of 5 years (i.e., $t_i \in \{2000, 2005, \dots, 2100\}$). The time horizon of each optimization is set to 2400 in order to account for the inertia of the climate system and ensure that emissions paths observing the guardrails in the 21st century do not violate them in the centuries to follow. For the numerical solutions of the optimization problems the GAMS package (General Algebraic Modelling System; Brooke et al. 1992) is employed. Fig. 1 illustrates the algorithm for the calculation of emissions corridors by displaying paths maximizing emissions in the years 2020, 2060, and 2100.

2.2 Specification of guardrails

In specifying the guardrail pertinent to the THC we take advantage of the fact that in our box model, similarly to other models, a well-defined threshold exists beyond which the circulation shuts down (Stocker and Schmittner 1997; Rahmstorf and Ganopolski 1999; Zickfeld et al. 2004). The exact value of such a threshold, if it exists in nature, is very difficult to determine. It can be shown analytically that in equilibrium the critical flow (i.e. the flow strength below which the circulation cannot be sustained) corresponds to half the equilibrium volume flux (or “overturning”) without freshwater forcing (Rahmstorf 1996) and is given as 11.3 Sv ($1 \text{ Sv} = 10^6 \text{ m}^3 \text{ s}^{-1}$) in our four-box model. In the transient case this picture changes slightly as the critical threshold is dependent upon the rate of climate change. We account for this transient effect by specifying the minimum admissible overturning m_{min} as 10 Sv. The guardrail constraining the THC strength is then cast

as:

$$m(t) \geq m_{min} = 10 \text{ Sv} \quad \forall t \in [t_0, t_{end}]. \quad (1)$$

In the course of a sensitivity analysis we tighten this constraint by requiring a minimum admissible THC overturning, expressed in terms of a maximum admissible weakening relative to the present-day value. The assumption of stricter guardrails is justified since already a weakening of the THC may be perceived as an intolerable outcome. In fact, it is conceivable that gradual THC changes trigger singular responses along the impact chain.

The socio-economic guardrails are intended to ensure that minimum requirements concerning economic development are met. In this study, the expectations about the socio-economically acceptable pace of emissions reductions are expressed in a simplified way by two conditions concerning the flexibility of emissions paths (Kriegler and Bruckner 2004). The first specifies the maximum feasible rate of emissions reductions r :

$$g(t) \geq -r \quad \forall t \in [t_0, t_{end}] \quad \text{with } g(t) := \dot{E}(t)/E(t), \quad (2)$$

where $E(t)$ denotes industrial CO₂ emissions.

The maximum emissions reduction rate r can be related to two major drivers of anthropogenic CO₂ emissions: the future level of economic activity and the future state of technology, determining both energy-use efficiency and technological options for energy generation. In the short term, r is determined by the existing energy infrastructure, which has an average turnover time of several decades. In the long run, it is determined by global energy demand. In the literature, estimates of the maximum feasible emis-

sions reduction rate r range from 0.5 to 3% per year (for a review cf. Alcamo and Kreileman 1996). After a detailed analysis of scenarios of technological change in the energy sector, Alcamo and Kreileman (1996) conclude that “in order to achieve global annual emissions reduction rates of more than 2%, substantial policy measures are required, even in the case of optimistic assumptions on technological change. ... It is therefore highly uncertain that rates of around 2% per year or higher can be maintained over such long periods of time [i.e., from 2010 to 2100]”. For our analysis, we have chosen a default value of 1.5% per year.

The second condition addresses socio-economic inertia by imposing a smoothness constraint on the transition to a decarbonizing economy (i.e., an economy where carbon emissions decrease in absolute terms). This is achieved by requiring a minimum time span t_{trans} for switching from today’s economic regime with increasing emissions to a regime where emissions decrease with the maximum reduction rate r . This constraint is motivated by evidence that emissions pathways allowing for a more gradual near-term transition away from carbon-venting fuels result in lower mitigation costs. One reason for this is the turnover time of the energy converting capital stock (e.g., power plants, buildings, transport systems). Another reason is that the availability of low-cost technological options depends on investments into “research and development” (R&D) and on “learning by doing” (Edenhofer et al. 2006). Watson et al. (1996), for example, report that the time required to put in place optimal technology for deep cuts in CO₂ corresponds to approximately 50 years. We use a default minimum transition time t_{trans} of 20 years, which may thus be considered as a rather weak

constraint.

Finally, we introduce a ‘monotony’ condition which allows growing CO₂ emissions to be followed by a reduction period, but not viceversa. For technical reasons we formulate this constraint even stronger by requiring that the emissions growth rate g decreases monotonously in time, with a maximum emissions growth rate g_0 in the year 2005. As pointed out in Kriegler and Bruckner (2004), this constraint is rather strong as it excludes emissions trajectories where the emissions growth rate itself grows after 2005. This would be the case, e.g., for emissions scenarios which assume a switch to coal after the exploitation of oil and gas reserves, as is the case in some of the SRES emissions scenarios (Nakićenović and Swart 2000). The majority of these scenarios, however, complies with the constraint.

We combine the ‘monotony’ condition and the constraint on the transition time into a single inequality:

$$-\frac{g_0 + r}{t_{trans}} \leq \dot{g}(t) \leq 0 \quad \forall t \in [t_0, t_{end}]. \quad (3)$$

Note that for vanishing transition times t_{trans} the change in the growth rate g is almost unlimited from below, allowing for a sudden switch in the emissions pathway (cf. Fig. 10).

3 Results

In the following, we present emissions corridors compatible with the goal of reducing the risk of THC collapse while keeping the pace of GHG mitigation

at a bearable level. First, we show the emissions corridor for standard (i.e. ‘best guess’) model settings (section 3.1). We then discuss the results of a sensitivity analysis where key uncertain model parameters, such as climate and North Atlantic hydrological sensitivity (section 3.2), emissions of non-CO₂ greenhouse gases (section 3.3) and sulfur dioxide (section 3.4), are varied sequentially. Lastly, we explore the dependence of the shape of the emissions corridor on the guardrails (i.e. minimum intensity of the THC, maximum emissions reduction rate, minimum transition time towards a decarbonizing economy; sections 3.5 and 3.6).

The standard values of the uncertain parameters as well as the ranges within which they are varied in the course of the sensitivity analysis are given in Table 1. In its standard setup, the climate model ICM is calibrated such that a doubling of CO₂ concentrations results in an asymptotic warming (which defines the equilibrium climate sensitivity $T_{2\times CO_2}$) of 2.5 °C (Bruckner et al. 2003). As best guess value for the North Atlantic hydrological sensitivity, in the following denoted as h , we adopt a value in the middle of the plausible range of 0.01–0.05 Sv°C⁻¹ (for a justification of this range cf. Rahmstorf and Ganopolski 1999).

For the calculation of emissions corridors we need to specify scenarios for the CO₂ emissions from land-use change (recall that the control variable are energy-related CO₂ emissions only) and emissions of non-CO₂ greenhouse gases and aerosols. For emissions of these gases during the 21st century we make use of the scenarios described in the IPCC Special Report on Emissions Scenarios (SRES; Nakićenović and Swart 2000). It is assumed that CO₂ emissions from land-use change and emissions of non-CO₂ greenhouse

Parameter	Standard value	Range
Climate sensitivity:		
$T_{2\times CO_2}$	2.5 °C	1.5 – 4.5, 7.7 – 9.4 °C
Hydrological sensitivity:		
h	0.03 Sv°C ⁻¹	0.01 – 0.05 Sv°C ⁻¹
Guardrails:		
m_{min}	10 Sv	60 – 90% $m(2000)$
r	0.015 yr ⁻¹	0.005 – 0.025 yr ⁻¹
t_{trans}	20 yrs	0 – 40 yrs
Non-CO ₂ GHGs :		
emissions scenario	mean of B1, B2, A1B, A2	B1, B2, A1B, A2
Desulfurization rate :		
ds	1.5% yr ⁻¹	0 – 3% yr ⁻¹

Table 1: Elements of the sensitivity analysis. 1 Sv corresponds to $10^6 \text{m}^3 \text{s}^{-1}$.

gases follow the average of the four “marker” scenarios (i.e., the average of scenarios B1, B2, A1B and A2) until 2100. From 2100 until 2400 (i.e., the time horizon of the optimization) these emissions are held constant. This is a rather strong assumption which can only be motivated by the lack of coherent scenarios for the time after 2100. Therefore, in section 3.3 we explore the sensitivity of the emissions corridors to alternative assumptions concerning long-term emissions of land-use change related CO₂ and non-CO₂ greenhouse gases.

In contrast to major non-CO₂ greenhouse gases such as CH₄ and N₂O which are to a large extent biogenic, sulfate aerosols originate mainly from the burning of fossil fuels. Therefore, it is reasonable to assume that SO₂ emissions $E(SO_2, t)$ are linked to the control variable, i.e., energy-related CO₂ emissions $E(CO_2, t)$. Because of the increasing control of sulfur emis-

sions by end-of pipe technologies due to the recognition of their negative effects on human health, food production and ecosystems, it can be assumed that over the long term SO_2 emissions will become independent from CO_2 emissions. This assumption is implemented in our model by introducing a so-called “desulfurization rate” ds :

$$\frac{E(SO_2, t)}{E(SO_2, t')} = \frac{E(CO_2, t)}{E(CO_2, t')} (1 - ds)^{dt}, \quad (4)$$

where $t' < t$ and $dt = t - t'$. As standard value we assume a globally averaged desulfurization rate of 1.5% per year.

3.1 Emissions corridor for standard parameter values

The emissions corridor for standard parameter settings is displayed in Fig. 1, along with selected emissions paths to illustrate its internal structure. The corridor boundaries demarcate emissions limits beyond which either the THC collapses or the socio-economic guardrails are violated. It must be emphasized that emissions corridors impose only a necessary condition on the admissibility of a particular emissions path, implying that not every arbitrarily selected path within the corridor is necessarily admissible (Bruckner et al. 1999). For example, the upper boundary of the corridor can be reached in 2060 only if emissions remain far inside the corridor for several decades in the first half of the 21st century.

For purpose of reference, Fig. 1 also displays representative low and high CO_2 emissions scenarios (SRES marker scenario B1 and A2, respectively; Nakićenović and Swart 2000). Our results indicate that for ‘best guess’

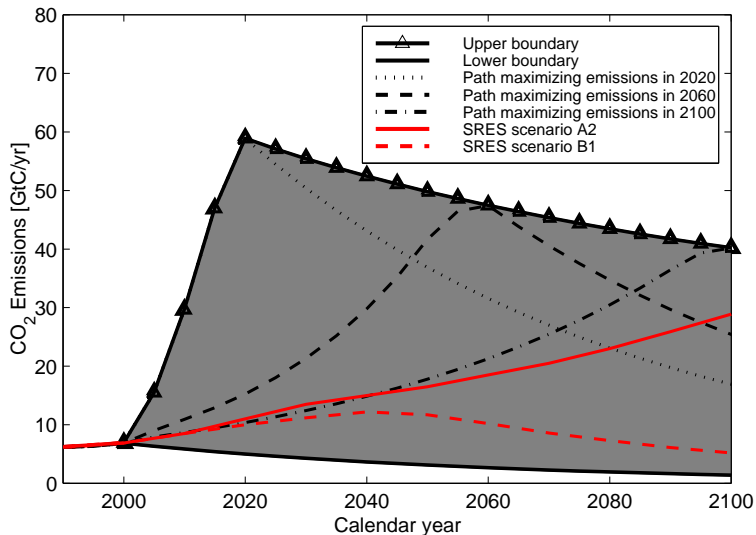


Figure 1: Emissions corridor – the shaded area between upper and lower boundaries – for standard parameter settings (cf. Table 1). For illustration of the underlying algorithm we show paths maximizing CO₂ emissions in 2020, 2060, and 2100. For reference, we also display representative low and high emissions scenarios (SRES marker scenarios B1 and A2, respectively).

parameter values the emissions corridor is wider than the range spanned by the SRES marker scenarios. This result might suggest that no immediate mitigation effort would be necessary in order to preserve the THC. In the following, however, we show that this result is very sensitive to the specific assumptions concerning climate and hydrological sensitivity.

Fig. 2 illustrates the constraints which the guardrails impose on CO₂ concentrations and global mean temperature. Fig. 2a shows the paths maximizing emissions in the years 2020, 2060 and 2100. Figs. 2b–d display the resulting CO₂ concentrations, changes in global mean temperature and thermohaline overturning strength. It is evident that in order to keep the THC within the guardrails (i.e., above the critical flow of 10 Sv), the change

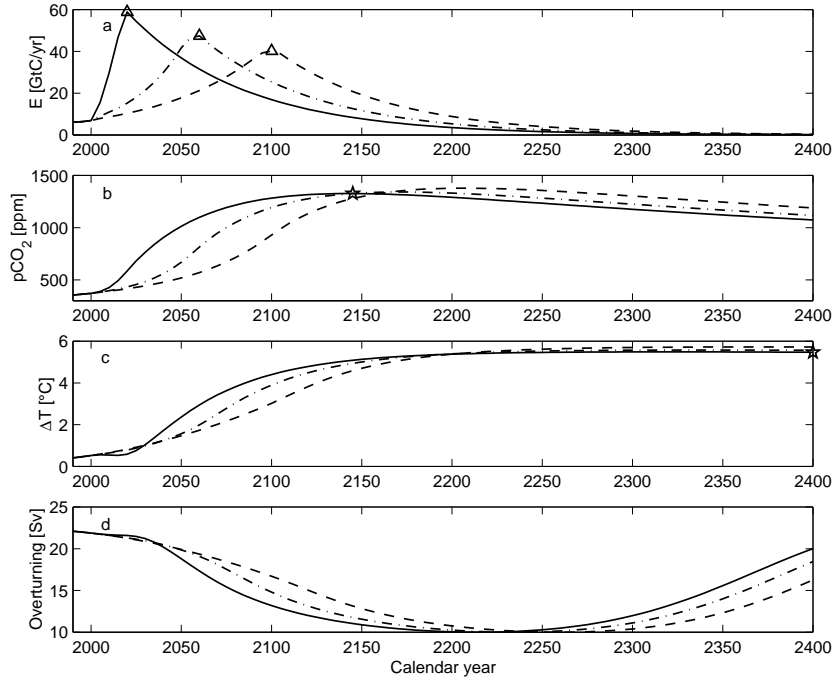


Figure 2: a) Paths maximizing CO₂ emissions in 2020, 2060, 2100 (solid, dashed-dotted and dashed lines, respectively). The triangles mark the points (maxima) that determine the upper corridor boundary in Fig. 1. b) CO₂ concentrations resulting from the emissions paths in a). c) Changes in global mean temperature relative to 1850 (under inclusion of the radiative forcing from non-CO₂ greenhouse gases and aerosols). d) Thermohaline overturning strength. The stars in b) and c) denote the values of maximum CO₂ concentrations (pCO_2^{max}) and stabilization temperature (T^{2400}) for the path maximizing CO₂ emissions in 2020, respectively.

in global mean temperature has to be stabilized at 5.5 °C. This value is approached asymptotically, without an overshoot. The reason is that any temperature increment, even if sustained only over a short period, would lead to additional freshwater entering the North Atlantic and hence crossing of the THC threshold. In terms of CO₂ concentrations, stabilization at 5.5 °C requires a maximum of approximately 1300 ppm reached around 2140 and a linear decline thereafter. A notable feature is the considerable lag between the time of maximum CO₂ emissions and that of maximum weakening of the THC: the emissions paths peaking during the 21st century lead to transient THC responses reaching their minima about two centuries later.

3.2 Emissions corridors for different values of climate and North Atlantic hydrological sensitivity

In this section we present emissions corridors for different values of the climate and North Atlantic hydrological sensitivity. The latter are the principal uncertain physical parameters in our model. For the climate sensitivity $T_{2\times CO_2}$, the IPCC indicates an uncertainty range of 2.0 to 4.5 °C (Meehl and Stocker 2007). Note, however, that in a number of studies this uncertainty range is extended considerably towards higher values (Andronova and Schlesinger 2001; Knutti et al. 2002; Forest et al. 2002; Gregory et al. 2002; Piani et al. 2005; Hegerl et al. 2006; Forest et al. 2006; Knutti et al. 2006). A plausible range for the hydrological sensitivity encompasses the values 0.01–0.05 Sv°C⁻¹ (Rahmstorf and Ganopolski 1999). First, we discuss the sensitivity of the corridors separately for the two parameters. Later, we

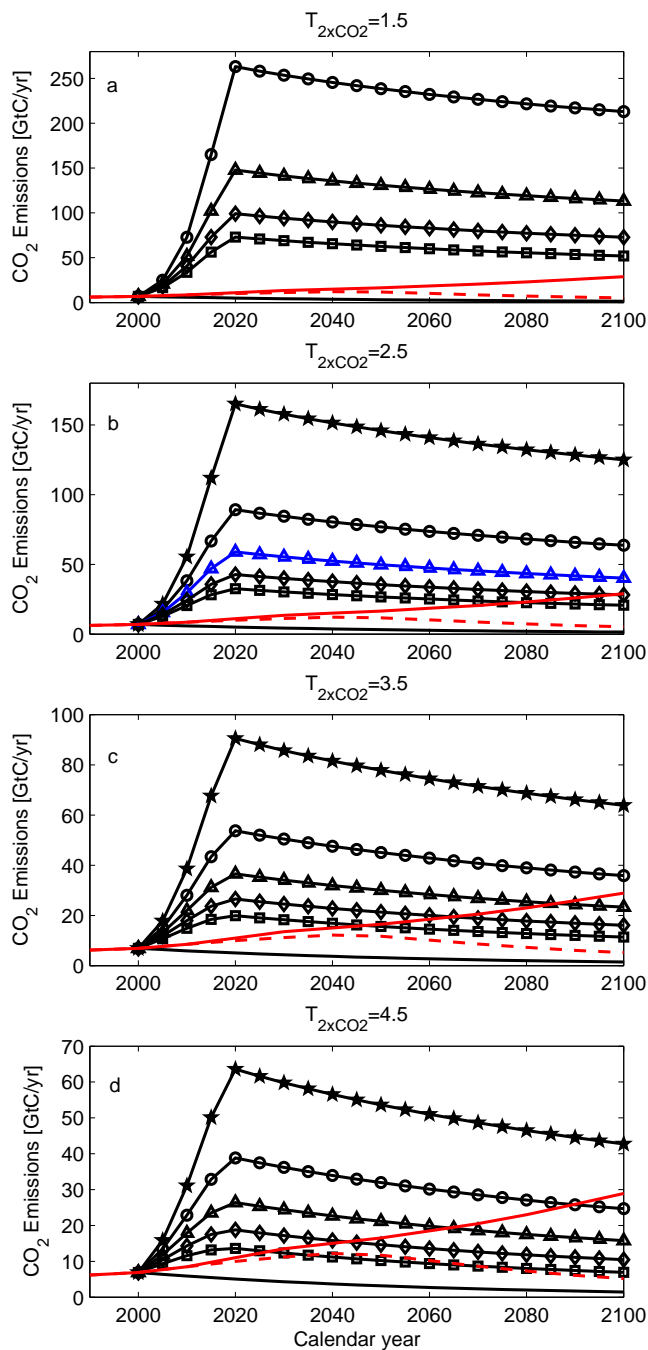


Figure 3: Emissions corridors for different values of climate and hydrological sensitivity (stars: $h = 0.01 \text{ Sv}^\circ\text{C}^{-1}$, circles: $h = 0.02 \text{ Sv}^\circ\text{C}^{-1}$, triangles: $h = 0.03 \text{ Sv}^\circ\text{C}^{-1}$, diamonds: $h = 0.04 \text{ Sv}^\circ\text{C}^{-1}$, squares: $h = 0.05 \text{ Sv}^\circ\text{C}^{-1}$). The corridor delimited by the boundary marked in blue corresponds to standard parameter values. For reference we display SRES emissions scenarios A2 (solid red line) and B1 (dashed red line). The corridor for the parameter combination $T_{2\times CO_2} = 1.5 \text{ }^\circ\text{C}$, $h = 0.01 \text{ Sv}/^\circ\text{C}$ is not shown since the associated allowable emissions exceed the domain of applicability of the coupled-carbon-cycle-plus-climate-model. Note that the figures have different scales.

present the results of an aggregated sensitivity analysis whereby we varied both parameters simultaneously.

Our findings indicate a strong sensitivity of the emissions corridor on the climate sensitivity parameter (cf. the curves marked by triangles in Fig. 3a–d). For a value of 1.5 °C, the corridor widens significantly (by 250%¹) relative to the corridor for standard parameter assumptions, such that its upper boundary is far from being touched by any of the SRES emissions scenarios for the 21st century. For climate sensitivities of 3.5 and 4.5 °C, the corridor shrinks relative to the standard case (by 38% resp. 55%), and the high reference emissions scenario (SRES marker scenario A2) crosses the upper corridor boundaries in the second half of the 21st century (cf. also Table 2). Note that the change in the width of the corridor is due entirely to the shift in the position of the upper boundary. The lower boundary remains unaffected by the climate sensitivity as it is solely determined by the maximum emissions reduction rate r .

It should be emphasized that a transgression of the corridor boundaries does not imply an immediate collapse of the THC: because of the inertia of the ocean, the actual event occurs centuries after it is triggered (Fig. 4). Once the corridor boundaries are transgressed, however, a collapse of the THC is inevitable.

The width of the emissions corridor is also largely dependent on the value of the North Atlantic hydrological sensitivity. Fig. 3b (which displays the corridors for the best guess climate sensitivity) indicates that for low values

¹As measure for the width of emissions corridors we take the maximum of the upper corridor boundary. Relative changes relate to this measure.

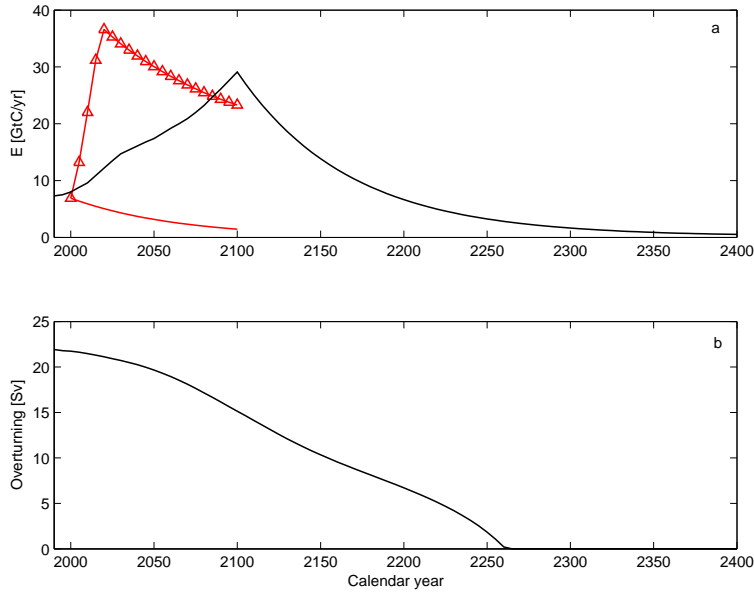


Figure 4: (a) CO₂ emissions following the SRES A2 scenario until 2100 and declining at 1.5% per year thereafter, (b) transient response of the THC to the emissions scenario displayed in (a) for $T_{2\times CO_2} = 3.5$ °C and $h = 0.03$ Sv/°C. Panel (a) also displays the emissions corridor for the 21st century for the above parameter settings. It is evident that the THC shuts down nearly 200 years after the A2 scenario crosses the upper corridor boundary.

of the hydrological sensitivity the corridor is much wider than the range spanned by the SRES marker scenarios, while for high parameter values the A2 scenario transgresses the upper corridor boundary in the second half of the 21st century.

In addition to the single parameter sensitivities, Fig. 3 illustrates the results of the aggregated sensitivity analysis, in which both parameters are varied simultaneously. If uncertainty in both parameters is considered, the range of allowable CO₂ emissions increases even more. For the ‘best case’ combination of climate and hydrological sensitivity ($T_{2\times CO_2}=1.5$ °C,

$T_{2\times CO_2}$ [$^{\circ}C$]	h [Sv/ $^{\circ}C$]					
	0.01	0.02	0.03	0.04	0.05	
1.5	–	14050	8050	5480	4100	E^{cum} [GtC]
	–	6650	3480	2240	1630	pCO_2^{max} [ppm]
	–	6.9	5.6	4.6	3.9	T^{2400} [$^{\circ}C$]
	–	–	–	–	–	t^{cross} [year]
2.5	8950	4960	3350	2470	1920	E^{cum} [GtC]
	3940	2010	1330	1000	820	pCO_2^{max} [ppm]
	9.2	6.9	5.5	4.5	3.9	T^{2400} [$^{\circ}C$]
	–	–	–	2100	2080	t^{cross} [year]
3.5	5030	3070	2140	1590	1220	E^{cum} [GtC]
	2040	1220	890	710	610	pCO_2^{max} [ppm]
	9.2	6.9	5.5	4.6	4.0	T^{2400} [$^{\circ}C$]
	–	–	2085	2065	2045	t^{cross} [year]
4.5	3600	2270	1580	1160	870	E^{cum} [GtC]
	1430	930	710	590	520	pCO_2^{max} [ppm]
	9.2	7.0	5.6	4.8	4.2	T^{2400} [$^{\circ}C$]
	–	2090	2065	2045	2025	t^{cross} [year]

Table 2: Maximum cumulative emissions in 2100 (E^{cum}), associated maximum CO₂ concentrations (pCO_2^{max}) and stabilization temperatures (T^{2400}) for the parameter constellations $T_{2\times CO_2} \in \{1.5, 2.5, 3.5, 4.5\} \times h \in \{0.01, 0.02, 0.03, 0.04, 0.05\}$. t^{cross} indicates the calendar year in which the SRES A2 scenario crosses the respective emissions corridor. For the parameter combination $T_{2\times CO_2} = 1.5$ $^{\circ}C$, $h = 0.01$ Sv/ $^{\circ}C$ no numbers are given since the associated allowable emissions exceed the domain of applicability of the coupled-carbon-cycle-plus-climate-model.

$h=0.02$ Sv/ $^{\circ}C$), the corridor is huge. For the ‘worst case’ combination of these parameters ($T_{2\times CO_2}=4.5$ $^{\circ}C$, $h=0.05$ Sv/ $^{\circ}C$), in contrast, the corridor is so tight that the low non-intervention scenario B1 crosses the upper corridor boundary in the first decades of the 21st century.

In order to convey an intuition of the maneuvering space for CO₂ emissions in the 21st century, we have calculated maximum admissible cumulative emissions in 2100 (E^{cum} ; Kriegler and Bruckner 2004) for all combinations

of climate and hydrological sensitivity (Table 2). Interestingly, for each parameter constellation the path maximizing cumulative emissions in 2100 corresponds to that maximizing annual CO₂ emissions in 2020. This is due to a peculiarity in the response of the carbon cycle: the faster a given amount of CO₂ is released to the atmosphere, the higher the fraction of atmospheric carbon which is taken up by the ocean (cf. Edmonds and Wise 1998). Along with E^{cum} Table 2 indicates the corresponding maximum CO₂ concentration (pCO_2^{max}) and stabilization temperature (T^{2400}) (for a definition of pCO_2^{max} and T^{2400} cf. Fig. 2 and related discussion). It must be emphasized, however, that these two values are given for illustrative purposes only, and are not central results of our analysis.

Table 2 illustrates that the sensitivity of E^{cum} to both climate and hydrological sensitivity is large and of comparable magnitude for both quantities. For the ‘best case’ combination of model parameters, for example, E^{cum} amounts to 14050 GtC, widely exceeding current estimates of carbon bound in fossil fuel reserves (1500–5000 GtC). In contrast, E^{cum} amounts to 870 GtC for the ‘worst case’ parameter combination. For comparison, the cumulative emissions in 2100 associated with the A2 and B1 scenarios amount to 1700 GtC and 920 GtC, respectively.

The stabilization temperature T^{2400} (i.e., the value at which GMT change has to be stabilized for a collapse of the THC to be avoided) ranges from 3.9 °C for the highest to 9.2 °C for the lowest value of the hydrological sensitivity. The values of T^{2400} are largely insensitive to climate sensitivity since the crucial quantity in determining the response of the THC, i.e., North Atlantic heat and freshwater forcing, depends solely on the amount of

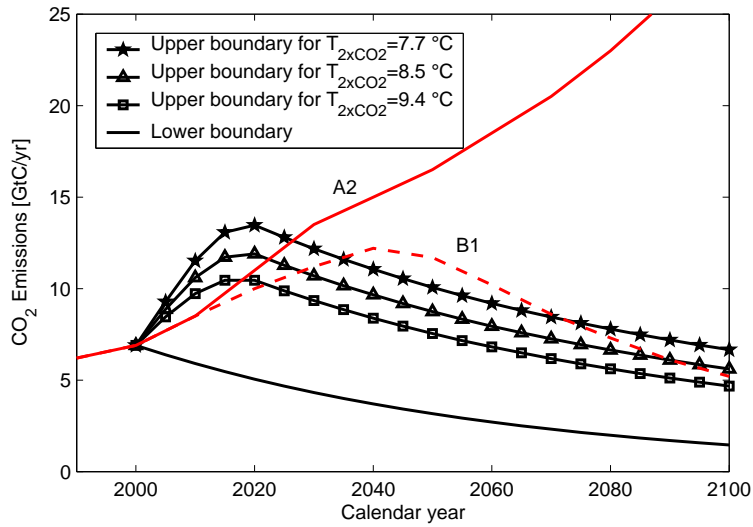


Figure 5: Emissions corridors for values of the climate sensitivity of 7.7 °C, 8.5 °C and 9.4 °C.

temperature increase and not on CO₂ concentrations. The slight differences arise because of transient effects associated with the sensitivity of the THC to the rate of temperature change (for higher $T_{2\times CO_2}$ the initial temperature response is slightly lower).

As mentioned earlier, recent studies suggest a much broader range for climate sensitivity than that indicated by the IPCC. For example, the 90% confidence interval of the distribution by Forest et al. (2002) ranges from 1.5 °C to 7.5 °C. In order to take this additional uncertainty into account, we have calculated emissions corridors for values for $T_{2\times CO_2}$ of 7.7 °C, 8.5 °C and 9.4 °C, which correspond to the 1, 2.5 and 5 percentiles of the distribution by Forest et al. (2002) (all other parameters are kept at their standard values). The results are displayed in Figure 5. As expected, the emissions

corridors are considerably tighter than those reported for climate sensitivities up to 4.5 °C. In all cases, both the SRES A2 and B1 emissions scenarios transgress the upper corridor boundary in the early decades of this century (A2: between 2015 and 2030; B1: between 2020 and 2035). It should be noted that for values of the hydrological sensitivity higher than 0.03 Sv/K no emissions corridors exist for the two highest values of climate sensitivity (8.5 °C and 9.4 °C). This implies that, given the amount of greenhouse gases already in the atmosphere and the inertia of the climate system, in these extreme cases the THC would be committed to collapse, unless the socio-economic guardrails were relaxed.

3.3 Sensitivity of the corridors to emissions of non-CO₂ greenhouse gases

In a set of simulations we investigated the influence of different assumptions concerning CO₂ emissions from land-use change and emissions of non-CO₂ greenhouse gases (GHGs) on the shape of the emissions corridors. We recall the standard assumption (cf. Table 1) that these emissions follow the average of the four SRES marker scenarios until 2100 and are held constant thereafter. In a first set of model runs we assume that emissions of CO₂ from land-use change and non-CO₂ GHGs follow one of the SRES marker scenarios B1, B2, A1B and A2 until 2100 and are constant thereafter. Subsequently, we explore the sensitivity to this constant assumption by projecting alternative storylines spanning the 22nd, 23rd and 24th century.

Fig. 6 displays emissions corridors for CO₂ from land-use change and non-CO₂ GHGs following the single SRES marker scenarios. The corridor

for our standard assumption is not displayed as it is almost identical to the corridor for the B2 scenario. The sensitivity of the corridor to the specific scenario is significant, although not as large as in the case of climate or hydrological sensitivity (cf. Fig. 3). For the B1 scenario, where emissions of the most influential non-CO₂ GHGs CH₄ and N₂O are lowest, the corridor is increased by 15% as compared to the standard case. In contrast, for the A2 scenario where emissions of CH₄ and N₂O increase strongly throughout the 21st century, the corridor is reduced by 20%. Note that the B2 scenario leads to a narrower corridor than the A1B scenario, contrarily to what one might expect on the basis of the respective CO₂ emissions (which are lower for the B2 than for the A1B scenario). The reason are much higher CH₄ emissions in the B2 scenario as compared to the A1B scenario. Note also that for non-CO₂ GHGs following the A2 scenario the reference CO₂ emissions scenario A2 approaches the upper corridor boundary rather closely. This means that if CO₂ *and* non-CO₂ GHGs will follow the A2 storyline, a collapse of the THC could be triggered in the first years of the 22nd century.

As already mentioned, the assumption that emissions of CO₂ from land-use change and non-CO₂ GHGs stay constant after 2100 can be motivated solely by the lack of more plausible alternatives. We therefore developed three different scenarios for emissions of these gases after 2100:

1. Emissions of non-CO₂ GHGs increase or decrease proportionally to energy-related CO₂ emissions².

²Ideally, only the energy-related fractions should be coupled to the control variable. Unfortunately, the SRES database does not allow one to discriminate between energy and non-energy related emissions of non-CO₂ GHGs.

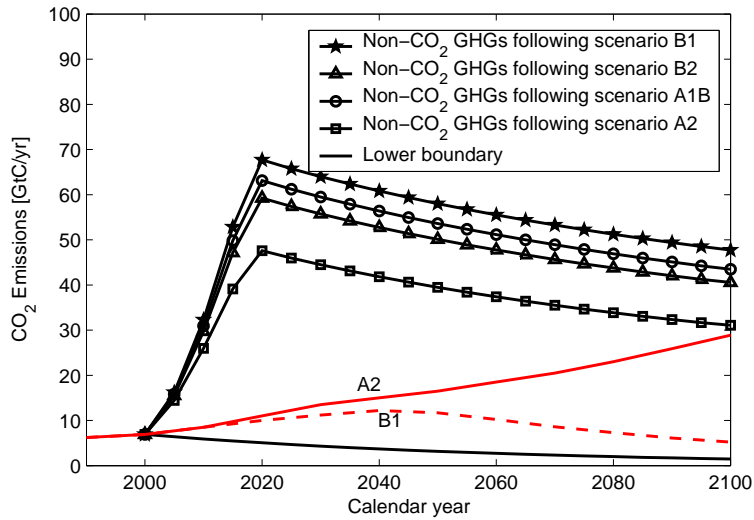


Figure 6: Emissions corridors for different assumptions regarding emissions of CO₂ from land-use change and non-CO₂ greenhouse gases.

2. Emissions of non-CO₂ GHGs follow the average of the SRES marker scenarios until 2100 and change in proportion to energy-related CO₂ emissions thereafter.
3. Emissions of non-CO₂ GHGs follow the average of the SRES marker scenarios until 2100 and then proceed according to their trend between 2050 and 2100.

In all three cases, emissions of CO₂ from land-use change follow our standard scenario. Note that in comparison to emissions of non-CO₂ GHGs such as CH₄ and N₂O land-use change emissions play only a minor role.

In a set of experiments we explored the sensitivity of the emissions corridor to these alternative scenarios. The tightest corridor arises from sce-

nario 1: the area of the corridor is decreased by 16% compared to the standard case. The reason is that in this case emissions of non-CO₂ GHGs reach rather high values in the first half of the 21st century, as they are coupled to energy-related CO₂ emissions which are maximized in order to determine the upper corridor boundary. The largest corridor is generated by assuming scenario 2: the corridor is increased by 14% compared to the standard case. This increase is due to the fact that emissions of non-CO₂ GHGs decline rapidly after 2100 such that higher CO₂ emissions can be attained before 2100. Scenario 3 gives rise to a corridor which differs little compared to the corridor for standard assumptions. The reason is that non-CO₂ GHGs increase only slightly (CH₄, N₂O) or decrease (SF₆) during the second half of the 21st century.

3.4 Sensitivity of the corridors to SO₂ emissions

In the following we discuss the sensitivity of emissions corridors to different assumptions concerning sulfur dioxide (SO₂) emissions. We recall that these emissions are linked to energy-related CO₂ emissions (i.e., the control variable) assuming a globally averaged desulfurization rate ds of 1.5%. In the course of a sensitivity analysis, we vary this quantity between 0 and 3% per year. The resulting emissions corridors for $ds=0-2.5\%$ are displayed in Fig. 7 (the corridor for $ds=3\%$ is not displayed as it almost coincides with that for $ds=2.5\%$). We find that the width of the emissions corridor decreases with increasing desulfurization rate. This can be explained as follows: because of the short residence time of sulfate (SO₄) aerosols (which are produced by the oxidation of SO₂) in the atmosphere, high ds is associated with a fast

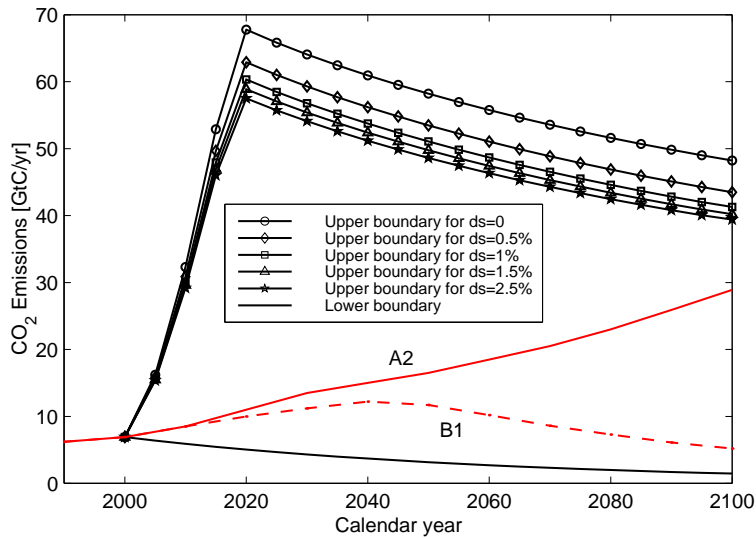


Figure 7: Emissions corridors for different assumptions concerning the desulfurization rate ds .

removal of the “aerosol mask” which, in turn, leads to faster and stronger warming³. This implies that the maximum CO₂ emissions that can be attained are lower in the case of a higher desulfurization rate. The specific dependence of the position of the upper corridor boundary on ds is a result of the sensitivity of the THC to the rate of climate change: the higher ds and thus the rate of temperature change, the lower the maximum temperature which can be attained if the THC is to be kept in the present-day mode of operation.

³The radiative forcing of sulfate aerosols is negative in sign. It consists of a “direct” and an “indirect” component. The direct effect is associated with the back-scattering of solar radiation; the first indirect effect is induced via changes in the optical properties of clouds. There are also other indirect effects, such as the influence of sulfate aerosols on cloud lifetime. ICM considers the direct and the first indirect effects.

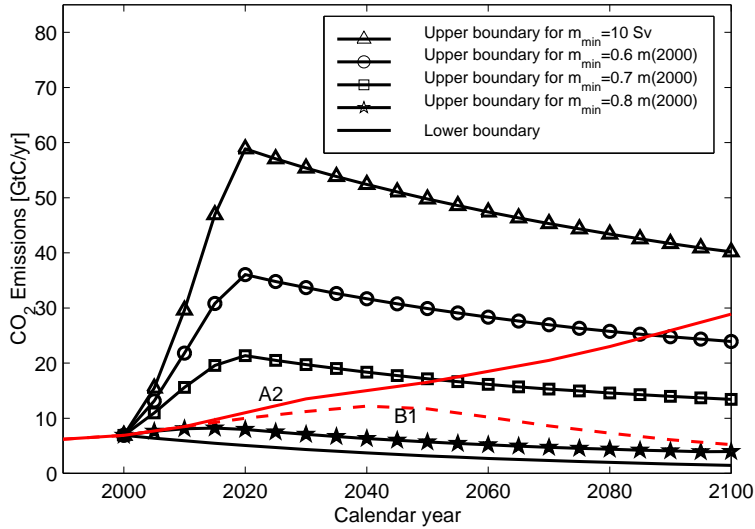


Figure 8: Emissions corridors for different assumptions about the THC guardrail expressed in terms of the minimum admissible circulation rate m_{min} .

3.5 Sensitivity of the corridors to the THC guardrail

So far, we have considered only a complete shutdown of the THC as a possibly unacceptable outcome that should be avoided in the sense of Article 2 of the UNFCCC. It is conceivable, however, that already a weakening of the THC (which is the response most models project for the 21st century; cf. Schmittner et al. 2005) might have considerable impacts, at least on the North Atlantic itself. Indeed, a slowdown of the THC would be associated with changes in the physical properties of the North Atlantic waters, such as, e.g., salinity, temperature, and mixed layer depth. This could affect marine ecosystems at all trophic levels with possible repercussions on the oceanic carbon cycle and fisheries (Schmittner et al. 2005; Vikebø et al. 2007; Obata 2007). Furthermore, it cannot be excluded that gradual changes in

the THC could force these systems across some threshold and hence generate singular responses. On these grounds, one might pursue a more ambitious policy target limiting changes in the THC to a specific amount of weakening relative to the present-day value.

In the following we discuss the sensitivity of the emissions corridor to the THC guardrail m_{min} , which is varied in the range of 60–90% of present-day circulation intensity $m(2000)$. This corresponds to a maximum admissible weakening of the THC of 40–10%. Our results suggest that the width of the emissions corridor depends strongly on the specific policy target. Fig. 8 shows that while the maneuvering space for the standard case $m_{min} = 10$ Sv is comfortable, it becomes considerably tighter if m_{min} is increased. Indeed, for $m_{min} = 0.7 \cdot m(2000)$ (i.e., a maximum admissible weakening of the THC of 30%) the high reference scenario A2 leaves the corridor in the mid-century. For $m_{min} = 0.8 \cdot m(2000)$ even the low non-intervention emissions scenario B1 leaves the corridor area in the early years of the 21st century, implying that it would be impossible to attain the target under a business-as-usual emissions regime. For $m_{min} = 0.9 \cdot m(2000)$ no emissions corridor exists. This implies that, given the amount of greenhouse gases already in the atmosphere and the inertia of the climate system, it is not feasible to limit changes in the THC to a 10% weakening under the prescribed socio-economic constraints. The emissions corridor could be ‘opened’ if mitigation options for non-CO₂ greenhouse gases were considered or the expectations about the socio-economically acceptable pace of CO₂ emissions reduction were relaxed (i.e., t_{trans} decreased and r increased; cf. next section).

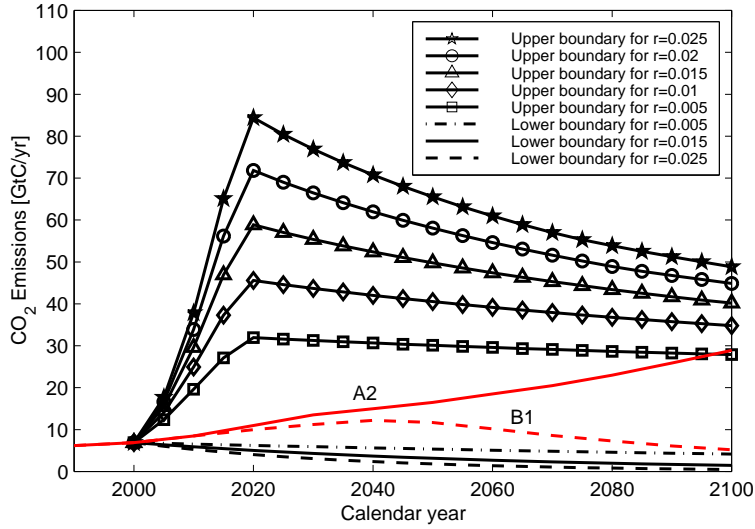


Figure 9: Emissions corridors for different assumptions about the maximum admissible emissions reduction rate r .

3.6 Sensitivity of the corridors to the socio-economic guardrails

Fig. 9 shows emissions corridors for different values of the maximum feasible emissions reduction rate r (cf. Eq. 2). Besides affecting the position of the upper boundary, r is the sole determinant of the shape of the lower corridor boundary: the latter corresponds to a path with emissions decreasing exponentially at a rate r . Although the overall width of the emissions corridor is mainly determined by the upper boundary, the shape of the lower boundary is crucial in the case of very tight emissions corridors. For the case $m_{min} = 0.8 \cdot m(2000)$ discussed in the previous section, for example, the corridor would vanish for a lower value of r (precisely for $r=0.005 \text{ yr}^{-1}$). The considerable increase of the width of the emissions corridors with increasing r can be explained with the higher flexibility associated with it. Indeed, the

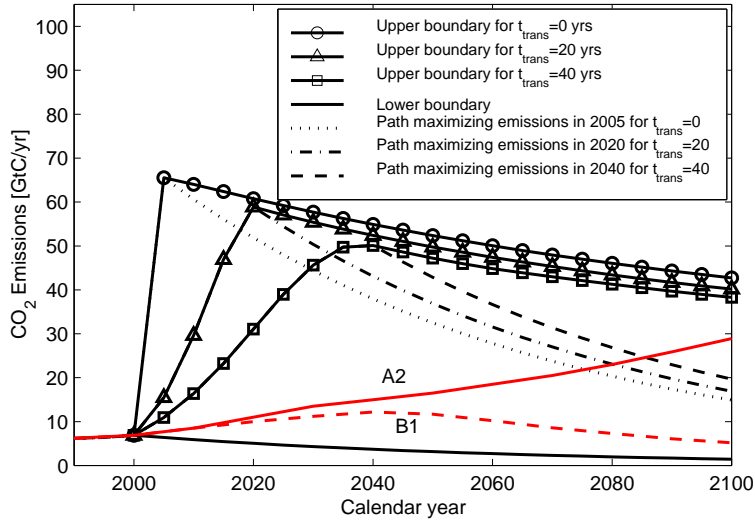


Figure 10: Emissions corridors for different assumptions about the transition pace towards a decarbonizing economy t_{trans} .

additional leeway is due to emissions paths which take advantage of the fast reduction capacity to attain high emissions in the short term.

Fig. 10 shows emissions corridors for different values of the transition time t_{trans} , which is an expression of the inertia characterizing the transition to a decarbonizing economy (cf. section 2.2). We found that t_{trans} determines the shape of the emissions corridor mainly in the first decades of the 21st century, while its effect is relatively small thereafter. The additional leeway for the case $t_{trans} = 0$ in relation to the standard case $t_{trans} = 20$, for example, is due to emissions paths which jump from maximally increasing to maximally decreasing emissions (i.e, from g_0 to r in Eq. 3; cf. Fig. 10).

Kriegler and Bruckner (2004) use the pertinent metaphor of a ships passage to illustrate the different role of the socio-economically motivated constraints and the climate guardrails in determining the shape of the emis-

sions corridors: “The latter affect the maneuvering space by determining the coast lines of the passage, while the former affect the maneuvering space by determining the maneuvering capacity of the ship”.

4 Summary and conclusions

The analysis presented in this paper aimed at identifying the leeway for action for climate policies committed to reducing the risk of THC collapse while considering expectations about the socio-economically acceptable pace of emissions reductions. We drew on the conceptual and methodological framework provided by the tolerable windows approach, which allowed us to operationalize the notion of a leeway in the form of emissions corridors.

The analytical tool employed consists of a dynamic box model of the thermohaline circulation (Zickfeld et al. 2004) coupled to the reduced-form ICLIPS climate model (ICM; Bruckner et al. 2003). This modelling framework allowed us to gain interesting insights into the dynamics of the coupled system, which was not possible in earlier studies using a static representation of the THC. A further advantage of the coupled ICM/THC model is its flexibility which allowed us to investigate the sensitivity of the results to a large number of uncertain quantities. These include physical parameters, such as the climate and hydrological sensitivities, and emissions of greenhouse gases and aerosols, and the chosen guardrails.

A shortcoming of our modeling framework so far is the crude representation of the socio-economic sphere. In a follow-up study, we have included an integrated energy-economy model which allows one to specify guardrails

concerning the costs of greenhouse gas (GHG) mitigation in domains that are more accessible to policymakers such as welfare or per capita income loss (Bruckner and Zickfeld 2006). Also, given the values at stake in the case of potentially abrupt and irreversible climate change, a risk assessment approach, allowing one to relate emissions levels to a probabilistic target (“limit the risk of a THC collapse to x%”), would be desirable (cf. Rahmstorf and Zickfeld 2005; Yohe et al. 2006; McInerney and Keller 2007). Such a risk analysis will also be the subject of a follow-up paper.

Results obtained within our modeling framework indicate that for the ‘best guess’ choice of model parameters, the CO₂ emissions corridor is larger than the range spanned by the SRES emissions scenarios for the 21st century, implying that under these circumstances short-term mitigation efforts are not required to preserve the THC. An extensive sensitivity analysis, however, indicates that this finding is largely dependent upon the specific choice of climate and North Atlantic hydrological sensitivities and assumptions about emissions of non-CO₂ greenhouse gases and aerosols.

Uncertainty in the climate sensitivity $T_{2\times CO_2}$ by a factor of three introduces even greater uncertainty in the allowable CO₂ emissions. As a consequence, for a climate sensitivity of 1.5 °C the corridor is much wider than the range spanned by the SRES emissions scenarios, while for high values (i.e., $T_{2\times CO_2} \geq 3.5$ °C) the A2 marker scenario transgresses the upper corridor boundary in the second half of this century. This indicates that if $T_{2\times CO_2}$ turns out to be in the middle of the IPCC range and emissions during the first decades of the 21st century will be high, CO₂ emissions will have to be reduced in the second half of this century for the THC to be

preserved.

A factor of five uncertainty in the North Atlantic hydrological sensitivity propagates onto a similar uncertainty in the width of the emissions corridor. Similarly to climate sensitivity, this implies a large range in the required CO₂ emissions reduction: from doing nothing in the case of low hydrological sensitivity to notable efforts in the second half of the 21st century in the case of high hydrological sensitivity and high reference CO₂ emissions.

Given that uncertainties in climate and hydrological sensitivity combine to an overall uncertainty range, we performed an aggregated analysis by varying both parameters simultaneously. Assuming ‘optimistic’ (i.e., low) values of both sensitivities, the resulting emissions corridor is huge: the associated cumulative emissions in the year 2100 of about 14000 GtC widely exceed current estimates of carbon bound in fossil fuel reserves (1500–5000 GtC). In contrast, if we assume high values of both sensitivities, the corridor area becomes very tight (associated cumulative emissions in 2100 amounting to 900 GtC), so that already low non-intervention emissions scenarios such as the SRES B1 scenario transgress the upper corridor boundary in the early decades of this century.

Besides climate and hydrological sensitivity, the width of the corridors is affected by assumptions concerning emissions of non-CO₂ GHGs and aerosols. The influence of these factors, however, is much smaller than that of the climate and hydrological sensitivity parameters.

In addition to the “prognostic” uncertainties discussed so far, the width of the emissions corridor is affected by the “normative” uncertainties. These reflect the subjectivity in the judgment of what may be considered unac-

ceptable. Firstly, we assumed a more ambitious THC guardrail by limiting the weakening of the THC to a 10–40% reduction relative to the present-day intensity. We found that the pursuit of a more ambitious THC target tightens the corridors considerably. As a consequence, no open corridor exists if a 10% weakening of the THC is to be avoided, implying that it would not be feasible to attain this target under the predefined socio-economic constraints. For a corridor to exist, these constraints could be relaxed, i.e., the maximum admissible emissions reduction rate r increased and/or the minimum admissible transition time t_{trans} decreased. This illustrates that a trade-off between THC and socio-economic guardrails may be required in the case of very tight emissions corridors. Concerning the sensitivity of emissions corridors to the socio-economically motivated guardrails, we found that the value of r significantly affects the corridor throughout the 21st century whereas the value of t_{trans} influences the corridor mainly in the first decades of this century.

In light of the huge uncertainty associated with the allowable range of CO₂ emissions and the values at stake, a precautionary attitude may seem advisable. This would require to keep global CO₂ emissions within the range spanned by the ‘worst case’ corridor, i.e., the corridor that arises under the most pessimistic assumptions about all pertinent parameters. The tightness of this corridor in our model emphasizes the necessity to abandon business-as-usual paths within the decades to come if the risk of a THC shutdown is to be kept low.

Acknowledgements

The first author thanks the German Federal Ministry for Education, Science, Research and Technology for financial support (grant no. 01LD0016).

References

- Alcamo, J. and E. Kreileman (1996). Emission scenarios and global climate protection. *Global Environmental Change* 6, 305–334.
- Andronova, N. and M. Schlesinger (2001). Objective estimation of the probability density function for climate sensitivity. *J. Geophys. Res.* 106(D19), 22,605–22,611.
- Bahn, O., L. Drouet, N. Edwards, A. Haurie, R. Knutti, S. Kypreos, T. Stocker, and J.-P. Vial (2006). The coupling of optimal growth and climate dynamics. *Clim. Change* 79(1–2), 103–119, doi: 10.1007/s10584-006-9108-4.
- Bahn, O., N. Edwards, R. Knutti, and T. Stocker (2007). Climate policy preventing an Atlantic thermohaline circulation collapse. *Clim. Change*. Submitted.
- Brooke, A., D. Kendrick, and A. Meeraus (1992). *GAMS: a user’s guide. Release 2.25*. Scientific Press.
- Bruckner, T., G. Hooss, H. Füßel, and K. Hasselmann (2003). Climate system modeling in the framework of the tolerable windows approach: the ICLIPS climate model. *Clim. Change* 56, 119–137.

- Bruckner, T., G. Petschel-Held, M. Leimbach, and F. Tóth (2003). Methodological aspects of the tolerable windows approach. *Clim. Change* 56, 73–89.
- Bruckner, T., G. Petschel-Held, F. Tóth, H. Füßel, C. Helm, M. Leimbach, and H. Schellnhuber (1999). Climate change decision support and the tolerable windows approach. *Env. Mod. Ass.* 4, 217–234.
- Bruckner, T. and K. Zickfeld (2006). Low risk emissions corridors for safeguarding the Atlantic thermohaline circulation. *Mitigation and Adaptation Strategies of Global Change*. Submitted.
- Caldeira, K., A. K. Jain, and M. I. Hoffert (2003). Climate sensitivity uncertainty and the need for energy without CO₂ emission. *Science* 299, 2052–2054.
- Dansgaard, W., S. Johnsen, H. Clausen, N. Dahl-Jensen, N. Gundestrup, C. Hammer, C. Hvidberg, J. Steffensen, A. Sveinbjornsdottir, J. Jouzel, and G. Bond (1993). Evidence for general instability of past climate from a 250-kyr ice-core record. *Nature* 364, 218–220.
- Edenhofer, O., C. Carraro, J. Koehler, and M. Grubb (Eds.) (2006). *Endogenous Technological Change and the Economics of Atmospheric Stabilization*, Volume 27 of *A Special Issue of The Energy Journal*. USA: International Association of Energy Economics.
- Edmonds, J. and M. Wise (1998). The value of advanced energy technologies in stabilizing atmospheric CO₂. In F. Tóth (Ed.), *Cost-Benefit Analyses of Climate Change*, pp. 87–104. Basel: Birkhäuser.

- Forest, C., P. Stone, A. Sokolov, M. Allen, and M. Webster (2002). Quantifying uncertainties in climate system properties with the use of recent climate observations. *Science* 295, 113–117.
- Forest, C. E., P. H. Stone, and A. P. Sokolov (2006). Estimated PDFs of climate system properties including natural and anthropogenic forcings. *Geophys. Res. Lett.* 33.
- Gregory, J., K. Dixon, R. Stouffer, A. Weaver, E. Driesschaert, M. Eby, T. Fichefet, H. Hasumi, A. Hu, J. Jungclaus, I. Kamenkovich, A. Levermann, M. Montoya, S. Murakami, S. Nawrath, A. Oka, A. Sokolov, and R. Thorpe (2005). A model intercomparison of changes in the Atlantic thermohaline circulation in response to increasing atmospheric CO₂ concentration. *Geophys. Res. Lett.* 32, L12703, doi:10.1029/2005GL023209.
- Gregory, J. and P. Huybrechts (2006). Ice-sheet contributions to future sea-level change. *Phil. Trans. R. Soc. Lond. A* 364, 1709–1731.
- Gregory, J., R. Stouffer, S. Raper, P. Stott, and N. Rayner (2002). An observationally based estimate of the climate sensitivity. *J. of Climate* 15(2), 3117–3121.
- Hansen, J. E. (2005). A slippery slope: How much global warming constitutes "dangerous anthropogenic interference"? *Clim. Change* 68, 269–279.
- Hegerl, G. C., T. J. Crowley, W. T. Hyde, and D. J. Frame (2006). Climate sensitivity constrained by temperature reconstructions over the past seven centuries. *Nature* 440, 1029–1032.

- Higgins, P. A. and M. Vellinga (2004). Ecosystem responses to abrupt climate change: teleconnections, scale and the hydrological cycle. *Climatic Change* 64, 127–142.
- Holland, M. M., C. M. Bitz, and B. Tremblay (2006). Future abrupt reductions in the summer Arctic sea ice. *Geophys. Res. Lett.* 33.
- Keller, K., B. M. Bolker, and D. F. Bradford (2004). Uncertain climate thresholds and optimal economic growth. *J. of Environmental Economics and Management* 48, 723–741.
- Keller, K., M. Hall, S. R. Kim, D. F. Bradford, and M. Oppenheimer (2005). Avoiding dangerous anthropogenic interference with the climate system. *Clim. Change* 73, 227–238.
- Keller, K., K. Tan, F. Morel, and D. Bradford (2000). Preserving the ocean circulation: implications for climate policy. *Clim. Change* 47, 17–43.
- Knutti, R., G. A. Meehl, M. R. Allen, and D. A. Stainforth (2006). Constraining climate sensitivity from the seasonal cycle in surface temperature. *J. Clim.* 19, 4224–4233.
- Knutti, R., T. Stocker, F. Joos, and G.-K. Plattner (2002). Constraints on radiative forcing and future climate change from observations and climate model ensembles. *Nature* 416, 719–723.
- Kriegler, E. and T. Bruckner (2004). Sensitivity analysis of emissions corridors for the 21st century. *Clim. Change* 66, 345–387.
- Leimbach, M. and T. Bruckner (2001). Influence of economic constraints

- on the shape of emission corridors. *Computational Economics* 18, 173–191.
- Lempert, R. J., M. E. Schlesinger, and J. K. Hammitt (1994). The impact of potential abrupt climate changes on near-term policy choices. *Clim. Change* 26, 351–376.
- Levermann, A., A. Griesel, M. Hofmann, M. Montoya, and S. Rahmstorf (2005). Dynamic sea level changes following changes in the thermohaline circulation. *Clim. Dyn.* 24, 347–354.
- Macdonald, A. and C. Wunsch (1996). An estimate of global ocean circulation and heat fluxes. *Nature* 382, 436–439.
- Manabe, S. and R. Stouffer (1988). Two stable equilibria of a coupled ocean-atmosphere model. *J. Climate* 1, 841–866.
- Manabe, S. and R. Stouffer (1993). Century-scale effects of increased atmospheric CO₂ on the ocean-atmosphere system. *Nature* 364, 215–218.
- Manne, A., R. Mendelsohn, and R. Richels (1995). MERGE: A model for evaluating regional and global effects of greenhouse gas reduction policies. *Energy Policy* 23, 17–34.
- Mastrandrea, M. and S. Schneider (2001). Integrated assessment of abrupt climatic changes. *Climate Policy* 1, 433–449.
- McInerney, D. and K. Keller (2007). Economically optimal risk reduction strategies in the face of uncertain climate thresholds. *Clim. Change*, doi: 10.1007/s10584-006-9137-z.
- Meehl, G. and T. Stocker (2007). Global climate projections. In S. Sa-

- lomon, D. Qing, and M. Manning (Eds.), *Climate Change 2007: The physical science basis – Contribution of Working Group I to the Fourth Assessment Report of the IPCC*, pp. 747–845. Cambridge: Cambridge University Press.
- Nakićenović, N. and R. Swart (2000). *Emissions scenarios*. Cambridge: Cambridge University Press.
- Nordhaus, W. (1994). *Managing the global commons: the economics of climate change*. Cambridge, MA: MIT Press.
- Obata, A. (2007). Climate-carbon cycle response to freshwater discharge into the North Atlantic. *J. Clim.*. In press.
- Oppenheimer, M. and R. B. Alley (2005). Ice sheets, global warming, and Article 2 of the unfccc. *Clim. Change* 68, 257–267.
- Oppenheimer, M. and A. Petsonk (2005). Article 2 of the UNFCCC: Historical origins, recent interpretations. *Clim. Change* 73, 195–226.
- Parry, M., T. Carter, and M. Hulme (1996). What is a dangerous climate change? *Global Environmental Change* 6(1), 1–6.
- Petschel-Held, G., H.-J. Schellnhuber, T. Bruckner, F. Tóth, and K. Hasselmann (1999). The tolerable windows approach: theoretical and methodological foundations. *Clim. Change* 41, 303–331.
- Piani, C., D. J. Frame, D. A. Stainforth, and M. R. Allen (2005). Constraints on climate change from a multi-thousand member ensemble of simulations. *Geophys. Res. Lett.* 32.
- Rahmstorf, S. (1995). Bifurcations of the Atlantic thermohaline circu-

- lation in response to changes in the hydrological cycle. *Nature* 378, 145–149.
- Rahmstorf, S. (1996). On the freshwater forcing and transport of the Atlantic thermohaline circulation. *Clim. Dyn.* 12, 799–811.
- Rahmstorf, S., M. Crucifix, A. Ganopolski, H. Goosse, I. Kamenkovich, R. Knutti, G. Lohmann, R. Marsh, L. A. Mysak, Z. Wang, and A. J. Weaver (2005). Thermohaline circulation hysteresis: A model intercomparison. *Geophys. Res. Lett.* 32, L23605, doi:10.1029/2005GL023655.
- Rahmstorf, S. and A. Ganopolski (1999). Long-term global warming scenarios computed with an efficient coupled climate model. *Clim. Change* 43, 353–367.
- Rahmstorf, S. and K. Zickfeld (2005). Thermohaline circulation changes: a question of risk assessment. *Clim. Change* 68, 241–247.
- Schaeffer, M., F. Selten, J. Opsteegh, and H. Goosse (2002). Intrinsic limits to predictability of abrupt regional climate change in IPCC SRES scenarios. *Geophys. Res. Lett.* 29(16), 10.1029/2002GL01524.
- Schellnhuber, H., W. Cramer, N. Nakicenovic, T. Wigley, and G. Yohe (Eds.) (2006). *Avoiding dangerous climate change*. Cambridge: Cambridge University Press.
- Schellnhuber, H.-J. (1997). Integrated assessment of climate change: regularity and singularity. Paper presented at the symposium ‘Climate impact research: Why, how and when?’, Berlin-Brandenburg Academy

of Sciences and German Academy Leopoldina, Berlin, October 28-29, 1997.

Schiller, A., U. Mikolajewicz, and R. Voss (1997). The stability of the North Atlantic thermohaline circulation in a coupled ocean-atmosphere general circulation model. *Clim. Dyn.* 13, 325–347.

Schmittner, A. (2005). Decline of the marine ecosystem caused by a reduction in the Atlantic overturning circulation. *Nature* 434, 628–633.

Schmittner, A., M. Latif, and B. Schneider (2005). Model projections of the North Atlantic thermohaline circulation for the 21st century assessed by observations. *Geophys. Res. Lett.* 32.

Smith, J., H.-J. Schellnhuber, and M. Mirza (2001). Lines of evidence for vulnerability to climate change: A synthesis. In J. McCarthy, O. Canziani, N. Leary, D. Dokken, and K. White (Eds.), *Climate Change 2001: Impacts, Adaptation and Vulnerability - Contribution of Working Group II to the Third Assessment Report of the IPCC*, pp. 914–967. Cambridge: Cambridge University Press.

Stocker, T. and A. Schmittner (1997). Influence of CO₂ emission rates on the stability of the thermohaline circulation. *Nature* 388, 862–865.

Stommel, H. (1961). Thermohaline convection with two stable regimes of flow. *Tellus* 13, 224–241.

Stouffer, R. and S. Manabe (2003). Equilibrium responds of thermohaline circulation to large changes in atmospheric CO₂ concentration. *Climate Dynamics* 20, 759–773.

- Stouffer, R. J., J. Yin, J. M. Gregory, K. W. Dixon, M. J. Spelman, W. Hurlin, A. J. Weaver, M. Eby, G. M. Flato, H. Hasumi, A. Hu, J. H. Jungclauss, I. V. Kamenkovich, A. Levermann, M. Montoya, S. Murakami, S. Nawrath, A. Oka, W. R. Peltier, D. Y. Robitaille, A. Sokolov, G. Vettoretti, and S. L. Weber (2006). Investigating the causes of the response of the thermohaline circulation to past and future climate changes. *J. Clim.* 19, 1365–1387.
- Tóth, F., G. Petschel-Held, and T. Bruckner (1998). Kyoto and the long-term climate stabilization. In *Proceedings of the OECD Workshop on Economic Modeling of Climate Change, Paris, September 17-18, 1998*.
- Vellinga, M. and R. Wood (2002). Global climatic impacts of a collapse of the Atlantic thermohaline circulation. *Clim. Change* 54, 251–267.
- Vellinga, M. and R. A. Wood (2007). Impacts of thermohaline circulation shutdown in the twenty-first century. *Clim. Change*, doi: 10.1007/s10584-006-9146-y.
- Vikebø, F. B., S. Sundby, B. Ådlandsvik, and O. H. Otterå (2007). Impacts of a reduced THC on growth, distribution and recruitment of Arcto-Norwegian cod. *Fisheries Oceanography*. In press.
- Watson, R., M. Zinyowera, and R. Moss (Eds.) (1996). *Climate Change 1995, Impacts, Adaptations and Mitigation of climate Change: Scientific-Technical Analysis – Contribution of Working Group II to the Second Assessment Report of the IPCC*. Cambridge: Cambridge University Press.
- Winguth, A., U. Mikolajewicz, M. Groger, E. Maier-Reimer, G. Schurg-

- ers, and M. Vizcaino (2005). Centennial-scale interactions between the carbon cycle and anthropogenic climate change using a dynamic Earth system model. *Geophys. Res. Lett.* 32.
- Wood, R., A. Keen, J. Mitchell, and J. Gregory (1999). Changing spatial structure of the thermohaline circulation in response to atmospheric CO₂ forcing in a climate model. *Nature* 399, 572–575.
- Yohe, G., M. E. Schlesinger, and N. G. Andronova (2006). Reducing the risk of a collapse of the Atlantic thermohaline circulation. *Integr. Assess. J.* 6(1), 57–73.
- Zickfeld, K. and T. Bruckner (2003). Reducing the risk of abrupt climate change: emissions corridors preserving the Atlantic thermohaline circulation. *Integrated Assessment* 4(2), 106–115.
- Zickfeld, K., A. Levermann, M. Morgan, T. Kuhlbrodt, S. Rahmstorf, and D. Keith (2007). Expert judgements on the response of the Atlantic meridional overturning circulation to climate change. *Clim. Change* 82(3–4), 235–265, doi: 10.1007/s10584-007-9246-3.
- Zickfeld, K., T. Slawig, and S. Rahmstorf (2004). A low-order model for the response of the Atlantic thermohaline circulation to climate change. *Ocean Dynamics* 54(1), 8–26.